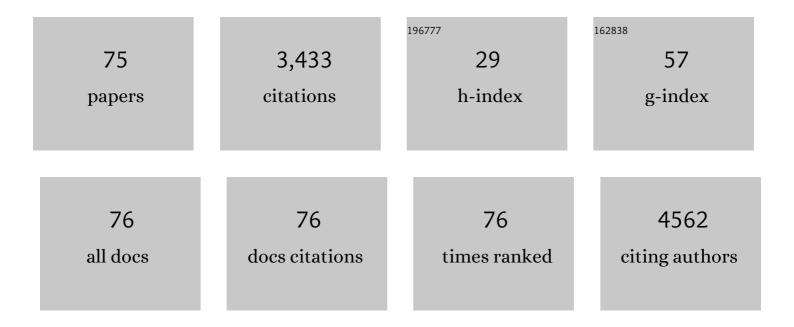
List of Publications by Year in descending order

Source: https://exaly.com/author-pdf/7148537/publications.pdf Version: 2024-02-01



#	Article	IF	CITATIONS
1	Charge Storage Behaviour of αâ€MoO ₃ in Aqueous Electrolytes – Effect of Charge Density of Electrolyte Cations. ChemElectroChem, 2022, 9, .	1.7	5
2	lsotropic and Anisotropic Flux Pinning Induced by Heavy-Ion Irradiation. IEEE Transactions on Applied Superconductivity, 2022, 32, 1-5.	1.1	5
3	The Role of Stacking Faults in the Enhancement of the <i>a-b</i> Plane Peak in Silver Ion-Irradiated Commercial MOD REBCO Wires. IEEE Transactions on Applied Superconductivity, 2022, 32, 1-5.	1.1	5
4	Effect of shearing prestrain on the hydrogen embrittlement of 1180ÂMPa grade martensitic advanced high-strength steel. Corrosion Science, 2022, 199, 110170.	3.0	10
5	In Operando Closed-cell Transmission Electron Microscopy for Rechargeable Battery Characterization: Scientific Breakthroughs and Practical Limitations. Nano Energy, 2022, 96, 107083.	8.2	7
6	Effect of cold deformation on the hydrogen permeation in a dual-phase advanced high-strength steel. Electrochimica Acta, 2022, 424, 140619.	2.6	5
7	Influence of hydrogen on the S–N fatigue of DP1180 advanced high-strength steel. Corrosion Science, 2022, 205, 110465.	3.0	4
8	Hydrogen-induced delayed fracture of a 1180â€⁻MPa martensitic advanced high-strength steel under U-bend loading. Materials Today Communications, 2021, 26, 101887.	0.9	3
9	ZIF-8 derived hollow carbon to trap polysulfides for high performance lithium–sulfur batteries. Nanoscale, 2021, 13, 11086-11092.	2.8	16
10	Prediction of Mechanical Properties of Wrought Aluminium Alloys Using Feature Engineering Assisted Machine Learning Approach. Metallurgical and Materials Transactions A: Physical Metallurgy and Materials Science, 2021, 52, 2873-2884.	1.1	22
11	Hydrogen fracture maps for sheared-edge-controlled hydrogen-delayed fracture of 1180 MPa advanced high-strength steels. Corrosion Science, 2021, 184, 109360.	3.0	18
12	Air electrodes and related degradation mechanisms in solid oxide electrolysis and reversible solid oxide cells. Renewable and Sustainable Energy Reviews, 2021, 143, 110918.	8.2	78
13	Nanoconfined Topochemical Conversion from MXene to Ultrathin Non‣ayered TiN Nanomesh toward Superior Electrocatalysts for Lithium‣ulfur Batteries. Small, 2021, 17, e2101360.	5.2	25
14	Hydrogen-induced fast fracture in notched 1500 and 1700 MPa class automotive martensitic advanced high-strength steel. Corrosion Science, 2021, 188, 109550.	3.0	21
15	Stable Interfaces in a Sodium Metal-Free, Solid-State Sodium-Ion Battery with Gradient Composite Electrolyte. ACS Applied Materials & Interfaces, 2021, 13, 39355-39362.	4.0	17
16	Sc, Ge co-doping NASICON boosts solid-state sodium ion batteries' performance. Energy Storage Materials, 2021, 40, 282-291.	9.5	52
17	Enhanced Safety and Performance of High-Voltage Solid-State Sodium Battery through Trilayer, Multifunctional Electrolyte Design. Energy Storage Materials, 2021, 41, 8-13.	9.5	23
18	Zn Electrodeposition by an <i>In Situ</i> Electrochemical Liquid Phase Transmission Electron Microscope. Journal of Physical Chemistry Letters, 2021, 12, 913-918.	2.1	24

#	Article	IF	CITATIONS
19	The role of functional materials to produce high areal capacity lithium sulfur battery. Journal of Energy Chemistry, 2020, 42, 195-209.	7.1	67
20	Catalyst–Electrolyte Interactions in Aqueous Reline Solutions for Highly Selective Electrochemical CO ₂ Reduction. ChemSusChem, 2020, 13, 304-311.	3.6	29
21	Separator coatings as efficient physical and chemical hosts of polysulfides for high-sulfur-loaded rechargeable lithium–sulfur batteries. Journal of Energy Chemistry, 2020, 44, 51-60.	7.1	47
22	Biomimetic Sn ₄ P ₃ Anchored on Carbon Nanotubes as an Anode for High-Performance Sodium-Ion Batteries. ACS Nano, 2020, 14, 8826-8837.	7.3	95
23	New Insights into the Degradation Behavior of Air Electrodes during Solid Oxide Electrolysis and Reversible Solid Oxide Cell Operation. Energy Technology, 2020, 8, 2000241.	1.8	6
24	Impact of Micropores and Dopants to Mitigate Lithium Polysulfides Shuttle over High Surface Area of ZIF-8 Derived Nanoporous Carbons. ACS Applied Energy Materials, 2020, 3, 5523-5532.	2.5	21
25	Hydrogen embrittlement of an automotive 1700 MPa martensitic advanced high-strength steel. Corrosion Science, 2020, 171, 108726.	3.0	42
26	Oriented nanoporous MOFs to mitigate polysulfides migration in lithium-sulfur batteries. Nano Energy, 2020, 75, 105009.	8.2	33
27	Catalyst–Electrolyte Interactions in Aqueous Reline Solutions for Highly Selective Electrochemical CO 2 Reduction. ChemSusChem, 2020, 13, 282-282.	3.6	2
28	A Study of Membrane Impact on Spatial Resolution of Liquid <i>In Situ</i> Transmission Electron Microscope. Microscopy and Microanalysis, 2020, 26, 126-133.	0.2	6
29	Effect of plastic strain damage on the hydrogen embrittlement of a dual-phase (DP) and a quenching and partitioning (Q&P) advanced high-strength steel. Materials Science & Engineering A: Structural Materials: Properties, Microstructure and Processing, 2020, 785, 139343.	2.6	20
30	Sn4P3@Porous carbon nanofiber as a self-supported anode for sodium-ion batteries. Journal of Power Sources, 2020, 461, 228116.	4.0	55
31	Sandwichâ€Like Ultrathin TiS ₂ Nanosheets Confined within N, S Codoped Porous Carbon as an Effective Polysulfide Promoter in Lithiumâ€Sulfur Batteries. Advanced Energy Materials, 2019, 9, 1901872.	10.2	186
32	Enhancing Oxygen Reduction Reaction Activity and CO ₂ Tolerance of Cathode for Low-Temperature Solid Oxide Fuel Cells by in Situ Formation of Carbonates. ACS Applied Materials & Interfaces, 2019, 11, 26909-26919.	4.0	35
33	Unveiling Lithium Roles in Cobaltâ€Free Cathodes for Efficient Oxygen Reduction Reaction below 600 °C. ChemElectroChem, 2019, 6, 5340-5348.	1.7	8
34	Evaluation of SrCo0.8Nb0.2O3-δ, SrCo0.8Ta0.2O3-δ and SrCo0.8Nb0.1Ta0.1O3-δ as air electrode materials for solid oxide electrolysis and reversible solid oxide cells. Electrochimica Acta, 2019, 321, 134654.	2.6	10
35	Recent advances in separators to mitigate technical challenges associated with re-chargeable lithium sulfur batteries. Journal of Materials Chemistry A, 2019, 7, 6596-6615.	5.2	173
36	Multifunctional Effects of Sulfonyl-Anchored, Dual-Doped Multilayered Graphene for High Areal Capacity Lithium Sulfur Batteries. ACS Central Science, 2019, 5, 1946-1958.	5.3	29

#	Article	IF	CITATIONS
37	Review on areal capacities and long-term cycling performances of lithium sulfur battery at high sulfur loading. Energy Storage Materials, 2019, 18, 289-310.	9.5	231
38	Cyclic Voltammetry in Lithium–Sulfur Batteries—Challenges and Opportunities. Energy Technology, 2019, 7, 1801001.	1.8	138
39	An Integrated Strategy towards Enhanced Performance of the Lithium–Sulfur Battery and its Fading Mechanism. Chemistry - A European Journal, 2018, 24, 18544-18550.	1.7	14
40	Non-enzymatic glucose sensor based on copper oxide and multi-wall carbon nanotubes using PEDOT:PSS matrix. Synthetic Metals, 2018, 245, 160-166.	2.1	43
41	In Situ Techniques for Developing Robust Li–S Batteries. Small Methods, 2018, 2, 1800133.	4.6	41
42	Porous Scandia-Stabilized Zirconia Layer for Enhanced Performance of Reversible Solid Oxide Cells. ACS Applied Materials & Interfaces, 2018, 10, 25295-25302.	4.0	18
43	Recent Progress on Advanced Materials for Solidâ€Oxide Fuel Cells Operating Below 500 °C. Advanced Materials, 2017, 29, 1700132.	11.1	257
44	Enhanced low-temperature critical current by reduction of stacking faults in REBCO coated conductors. Superconductor Science and Technology, 2017, 30, 074005.	1.8	13
45	A porous yttria-stabilized zirconia layer to eliminate the delamination of air electrode in solid oxide electrolysis cells. Journal of Power Sources, 2017, 359, 104-110.	4.0	33
46	Solidâ€Oxide Fuel Cells: Recent Progress on Advanced Materials for Solidâ€Oxide Fuel Cells Operating Below 500 °C (Adv. Mater. 48/2017). Advanced Materials, 2017, 29, 1770345.	11.1	97
47	Structure property relationships in a nanoparticle-free SmBCO coated conductor. Superconductor Science and Technology, 2016, 29, 065006.	1.8	11
48	New composites of nanoparticle Cu (I) oxide and titania in a novel inorganic polymer (geopolymer) matrix for destruction of dyes and hazardous organic pollutants. Journal of Hazardous Materials, 2016, 318, 772-782.	6.5	91
49	Relating Critical Currents to Defect Populations in Superconductors. IEEE Transactions on Applied Superconductivity, 2013, 23, 8001705-8001705.	1.1	9
50	Optimizing solid oxide fuel cell cathode processing route for intermediate temperature operation. Applied Energy, 2013, 104, 984-991.	5.1	24
51	Electrochemical characterization of La0.6Ca0.4Fe0.8Ni0.2O3â^'δ perovskite cathode forÂIT-SOFC. Journal of Power Sources, 2013, 239, 196-200.	4.0	22
52	Oxidation in ceria infiltrated metal supported SOFCs – A TEM investigation. Journal of Power Sources, 2013, 228, 75-82.	4.0	22
53	Modeling Degradation in SOEC Impedance Spectra. Journal of the Electrochemical Society, 2013, 160, F244-F250.	1.3	19
54	Oxygen Deficiency, Stacking Faults and Calcium Substitution in MOD YBCO Coated Conductors. IEEE Transactions on Applied Superconductivity, 2013, 23, 7200205-7200205	1.1	15

#	Article	IF	CITATIONS
55	Co-Electrolysis of Steam and Carbon Dioxide in Solid Oxide Cells. Journal of the Electrochemical Society, 2012, 159, F482-F489.	1.3	148
56	Efficient dual layer interconnect coating for high temperature electrochemical devices. International Journal of Hydrogen Energy, 2012, 37, 14501-14510.	3.8	39
57	Improved oxidation resistance of ferritic steels with LSM coating for high temperature electrochemical applications. International Journal of Hydrogen Energy, 2012, 37, 8087-8094.	3.8	20
58	High Performance Cathodes for Solid Oxide Fuel Cells Prepared by Infiltration of La0.6Sr0.4CoO3â^δ into Gd-Doped Ceria. Journal of the Electrochemical Society, 2011, 158, B650.	1.3	71
59	Cation inter-diffusion between LaMnO3 and LaCoO3 materials. Solid State Ionics, 2011, 202, 6-13.	1.3	32
60	Electrochemical characterisation of solid oxide cell electrodes for hydrogen production. Journal of Power Sources, 2011, 196, 4396-4403.	4.0	21
61	Durability of Solid Oxide Cells. Green, 2011, 1, .	0.4	63
62	Hydrogen and synthetic fuel production using pressurized solid oxide electrolysis cells. International Journal of Hydrogen Energy, 2010, 35, 9544-9549.	3.8	172
63	Glassâ€Phase Movement in Yttriaâ€Stabilized Zirconia/Alumina Composites. Journal of the American Ceramic Society, 2010, 93, 1494-1500.	1.9	2
64	Cathode–Electrolyte Interfaces with CGO Barrier Layers in SOFC. Journal of the American Ceramic Society, 2010, 93, 2877-2883.	1.9	103
65	Origin of Polarization Losses in Solid Oxide Electrolysis Cells under High Current Density. ECS Transactions, 2010, 28, 77-87.	0.3	4
66	Investigation of Failure Mechanisms in Ti Containing Brazing Alloys Used in SOFC/SOEC Environments. , 2010, , .		1
67	Solid Oxide Electrolysis Cells: Degradation at High Current Densities. Journal of the Electrochemical Society, 2010, 157, B1209.	1.3	275
68	Corrosion stability of ferritic stainless steels for solid oxide electrolyser cell interconnects. Corrosion Science, 2010, 52, 3309-3320.	3.0	100
69	Effect of alumina additions in YSZ on the microstructure and degradation of the LSM–YSZ interface. Solid State Ionics, 2009, 180, 984-989.	1.3	6
70	Synthesis and characterisation of macroporous Yttria Stabilised Zirconia (YSZ) using polystyrene spheres as templates. Microporous and Mesoporous Materials, 2009, 117, 395-401.	2.2	35
71	Effect of alumina additions on the anode electrolyte interface in solid oxide fuel cells. Journal of Power Sources, 2008, 179, 511-519.	4.0	9
72	Electrochemical Characterization of Planar Anode Supported SOFC with Strontium-Doped Lanthanum Cobalt Oxide Cathodes. ECS Transactions, 2008, 13, 285-299.	0.3	21

#	Article	IF	CITATIONS
73	Ultrahigh Electron Emissive Carbon Nanotubes with Nano-sized RuO2 Particles Deposition. Journal of Nanoparticle Research, 2007, 9, 1201-1204.	0.8	4
74	Analytical electron microscopy of proton exchange membrane fuel cells. Solid State Ionics, 2006, 177, 1649-1654.	1.3	3
75	Cobaltâ€doped Cu ₆ Sn ₅ lithiumâ€ion battery anodes with enhanced electrochemical properties. Nano Select, 0, , .	1.9	2